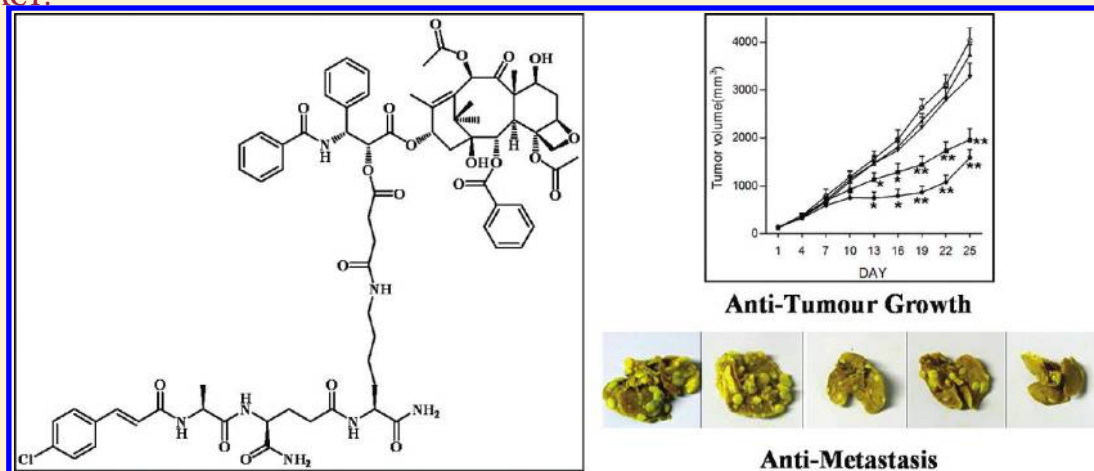ARTICLE

Conjugate (MTC-220) of Muramyl Dipeptide Analogue and Paclitaxel Prevents Both Tumor Growth and Metastasis in Mice

Yao Ma,[†] Nan Zhao,[†] and Gang Liu*

Institute of Materia Medica, Chinese Academy of Medical Sciences and Peking Union Medical College, 2A Nanwei Road, Xicheng District, Beijing 100050, P. R. China

S *Supporting Information*

ABSTRACT:

1 (MTC-220), a conjugate of paclitaxel and a muramyl dipeptide analogue, has been synthesized as a novel agent of dual antitumor growth and metastasis activities. In vitro and in vivo tests show that **1** retains its ability to inhibit tumor growth. It is superior to paclitaxel in its ability to prevent tumor metastasis in Lewis lung carcinoma and 4T1-tumor-bearing mice. The present studies indicate that **1** suppresses myeloid derived suppressor cell accumulation in the spleen and bone marrow of tumor-bearing mice and also represses inflammatory cytokines in tumor tissue. These results demonstrated that **1** could be a potential therapeutic and preventive agent for cancer growth and metastasis.

■ INTRODUCTION

Metastasis is the main cause of mortality in cancer patients, accounting for about 90% of deaths from solid tumors.[1] Data collected by the U.S. National Cancer Institute (NCI) show that approximately 10%–40% of cancer patients had detectable distant metastases at diagnosis and another 20%–37% of individuals are at high risk of metastasis.[2] However, current therapies have a limited impact at this stage. The combination of chemotherapy with immunotherapy is of increasing interest in various types of cancer to prevent drug resistance and tumor metastasis. Recently, the addition of immunotherapy agent muramyl tripeptide phosphatidy-lethanolamine (MTP-PE) to a chemotherapy regimen (ifosfamide, cisplatin, doxorubicin and methotrexate) resulted in a trend toward improved even-free survival (EFS) and a one-third reduction in the risk of death from an ultraorphan disease called osteosarcoma.[3,4]

Paclitaxel (Taxol), one of the most widely used chemother-apeutic agents, exerts its cytotoxic effect by arresting mitosis through microtubule stabilization.[5,6] More recent studies indicate that pacli-taxel also acts as a lipopolysaccharide (LPS) mimic in mice, binding

to Toll-like receptor 4 (TLR4)[7] and stimulating macrophages to release tumor necrosis factor α (TNF-α),[8] which has been shown to be a metastasis-promoting cytokine.[9,10] Although the effects of paclitaxel on human macrophages are controversial,[11,12] a number of reports[13–16] demonstrated that TLR-4 signaling negatively regulates paclitaxel chemotherapy and supports tumor progression and chemoresistance, promoting immune escape in human lung cancer and ovarian cancer. A clinical investigation[17] in 2002 reported that the levels of TNF-α and interleukin (IL)-1 were much higher in breast cancer patients than in health controls. After treatment with paclitaxel, TNF-α and IL-1 levels slightly decreased but never returned to the levels observed in the healthy group. All this evidence may explain why paclitaxel has limited utility in suppressing the metastatic spread of cancer cells in humans.
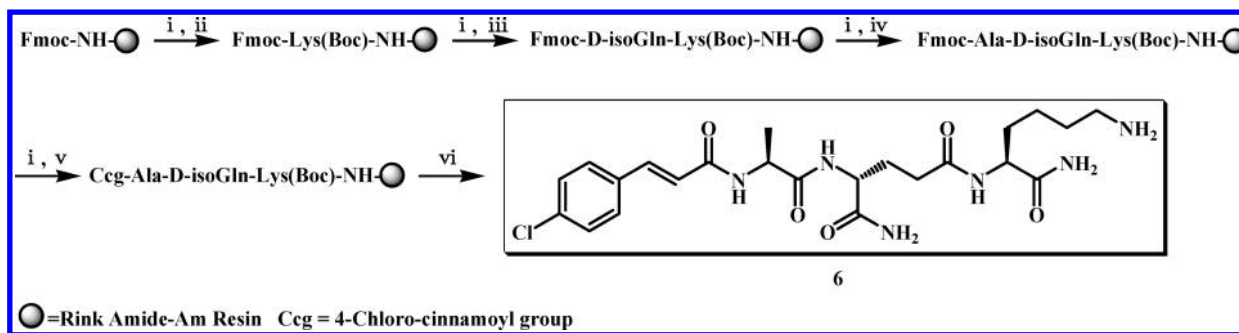
Muramyl dipeptide (MDP) and its analogues are immuno-modulators.[18–21] Our group previously designed and

Scheme 1. Preparation of Fmoc-isoGln-OH (5) in Solution[a]
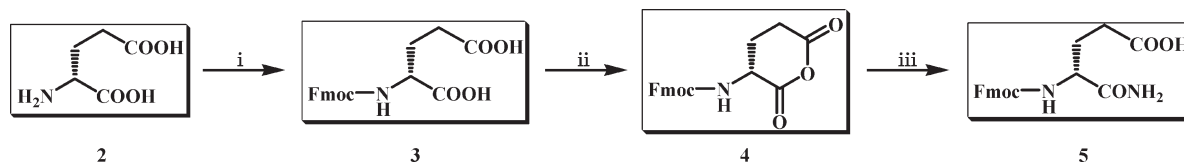
[a] Reagents and conditions: (i) Fmoc-OSu, 50% acetone/H_2O, rt, 3 days; (ii) DCC, THF, 0 °C to rt, 10 h; (iii) dry ammonia gas, THF, −10 °C, 1.5 h.

Scheme 2. Synthesis of MDA (6) on Solid Phase[a]

[a] Reagents and conditions: (i) 20% piperidine/DMF, rt, 1 h; (ii) Fmoc-Lys(Boc)-OH, HOBt, DIC, DMF, rt, 8 h; (iii) Fmoc-D-isoGln-OH, HOBt, DIC, DMF, rt, 12 h; (iv) Fmoc-Ala-OH, HOBt, DIC, DMF, rt, 8 h; (v) 4-chlorocinnamic acid, HOBt, DIC, DMF, rt, 8 h; (vi) 90% TFA/H_2O, rt, 2 h.

synthesized conjugates (MTCs) of MDP and paclitaxel at various linkage positions.[22] We have reported a conjugate (2′-O-MTC-01) that not only retains its cytotoxicity against most tumor cell lines but also has immunoenhancing capacity in vitro. Further experiments indicated 2′-O-MTC-01 is powerless to prevent metastasis of Lewis lung carcinoma (LLC) in mice, which may be caused by its consistent ability to induce inflammatory cytokines, especially TNF-α.[23] Continuous modifications of the MTCs have led to the identification of a novel compound, **1**. Herein, we demonstrate that **1** effectively inhibits tumor growth in nude mice and significantly prevents tumor metastasis in vivo. The current mechanistic studies indicate that **1** suppresses myeloid-derived suppressor cell (MDSC) accumulation in the spleen and bone marrow of tumor-bearing mice and also represses the mRNA levels for inflammatory cytokines including TNF-α in tumor tissue.

RESULTS

Chemical Synthesis of Compound 1. To synthesize **1**, a combination of solution-phase synthesis and solid-phase synthesis was performed. All synthetic steps included an improved Fmoc-isoGln-OH (**5**) preparation (Scheme 1) in solution, synthesis of MDA (**6**) on solid phase (Scheme 2), and a final **1** conjugation in solution (Scheme 3). This hybrid method allows us to obtain **1** with high efficacy (Figure 1).

1 Inhibits Tumor Growth in Vitro. In an initial approach to test the potential cytotoxic activity of **1**, we performed a 3-(4,5-dimethylthiazol-2-yl)-2,5-diphenyltetrazolium bromide (MTT) assay employing eight tumor cell lines: HCT-8 (human colon cancer), HeLa (human cervical cancer), A431 (human skin cancer), KB (human head and neck cancer), A2780 (human ovarian cancer), KeTr3 (human renal cancer), PC3M (human prostate cancer), and BGC-823 (human stomach cancer). Paclitaxel was included as a control. After treatment of cells for 72 h, **1** displayed strong cytotoxicity comparable with that of paclitaxel

(Supporting Information). In repeat experiments with the NCI60 cell line screen performed by the NCI Developmental Therapeutics Program (DTP), **1** was found to inhibit tumor cell growth with a mean GI_{50} of approximately 22 nM, with a number of cell lines exhibiting a GI_{50} of less than 10 nM (Figure 2).

1 Inhibits Tumor Growth in Nude Mice. The tolerated dose of **1** was determined in ICR mice. After intravenous (iv) injections at 112.5 mg/kg, **1** [formulated in DMSO/Cremophor/water at 5:5:90 (v:v:v)] was well tolerated with no apparent toxicity.

Because **1** significantly inhibited tumor cell growth in vitro, we further screened its effectiveness in xenograft models using human breast (MDA-MB-231, MCF-7), ovarian (A2780, ES-2), and lung (H460, A549, H1975) tumor cell lines. After implantation into the right flank region of nude mice, tumors were allowed to grow to an average volume of 100 mm^3 before beginning treatment with **1**. The results of each xenograft study are summarized in Table 1, and a representative result is shown in Figure 3. The treatment was well tolerated, and no apparent side effects or body weight loss were observed with the doses given. These data indicate that **1** was efficacious in inhibiting the growth of several tumor types in vivo, especially human breast tumor (MDA-MB-231, MCF-7) and lung cancer (H460, A549, H1975).

1 Inhibits the Growth and Metastasis of Transplanted Lewis Lung Carcinoma (LLC) Cells and Breast Cancer 4T1 Cells. To determine whether **1** has an antimetastatic effect in vivo, an LLC model was established in C57BL/6 mice. After a 15-day treatment, no discernible loss of body weight was observed in all treated groups. At the end of the experiment, the rates of inhibition of tumor growth and lung metastasis in the **1**-treated group (10 mg/kg) were 33.1% ($p < 0.01$) and 47.4% ($p < 0.05$), respectively, compared to the vehicle control group (Figure 4B). Although a similar tumor growth inhibition (26.2%) was measured in the paclitaxel-treated group (equimolar dose of **1**), no significant difference was found in lung metastasis nodule counts compared to the vehicle group (Figure 4A).

Scheme 3. Conjugation of Building Blocks To Prepare 1 in Solution[a]
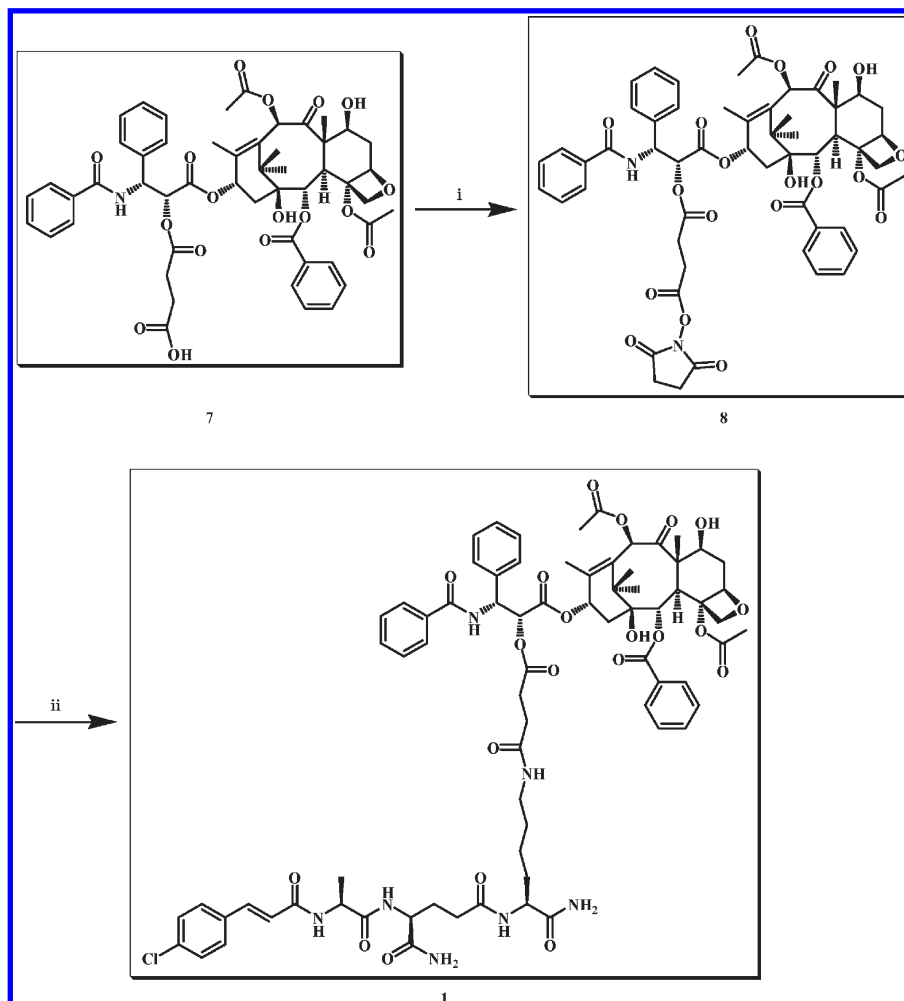
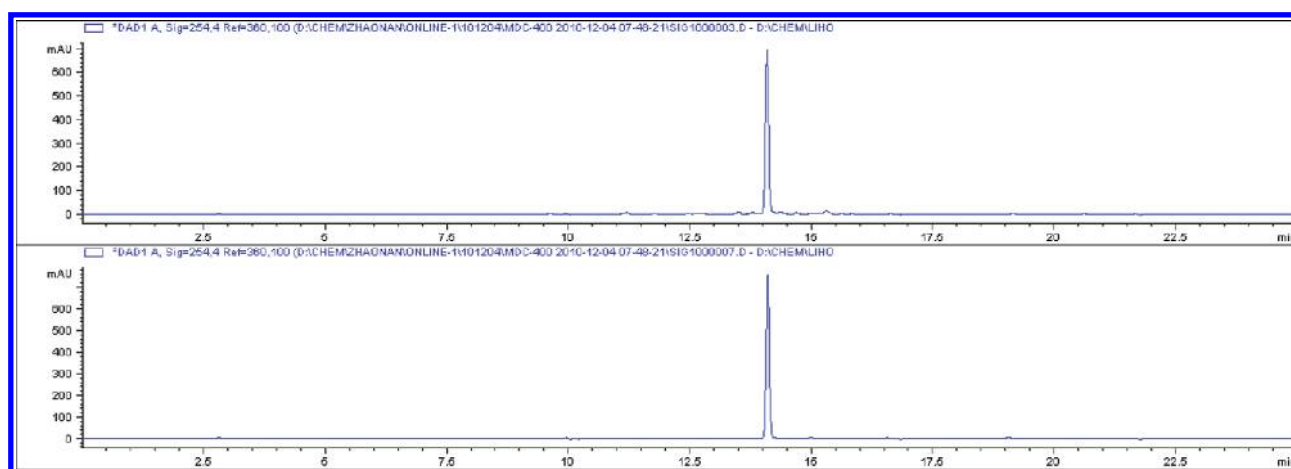[a] Reagents and conditions: (i) HOSu, EDC·HCl, DMSO, rt, 8 h; (ii) MDA, NMM, DMSO, rt, 30 min.

Figure 1. HPLC profiles of **1** at 254 nm UV wavelength: (top) crude **1**; (bottom) purified **1**.

We also tested the antimetastatic effect of **1** in the highly invasive and metastatic 4T1 mammary carcinoma model. The tumor-bearing mice were treated with paclitaxel at 3 mg/kg (an equimolal dose of **1** at 5 mg/kg) or **1** at dose of 2.5, 5, or 10 mg/kg. Again, no discernible loss of body weight was observed in all treated groups even after a prolonged therapy for 28 days (Figure 5A). Treatments with **1** exhibited inhibition of tumor growth, and the rates were 27.4% (2.5 mg/kg), 33.5% (5 mg/kg),
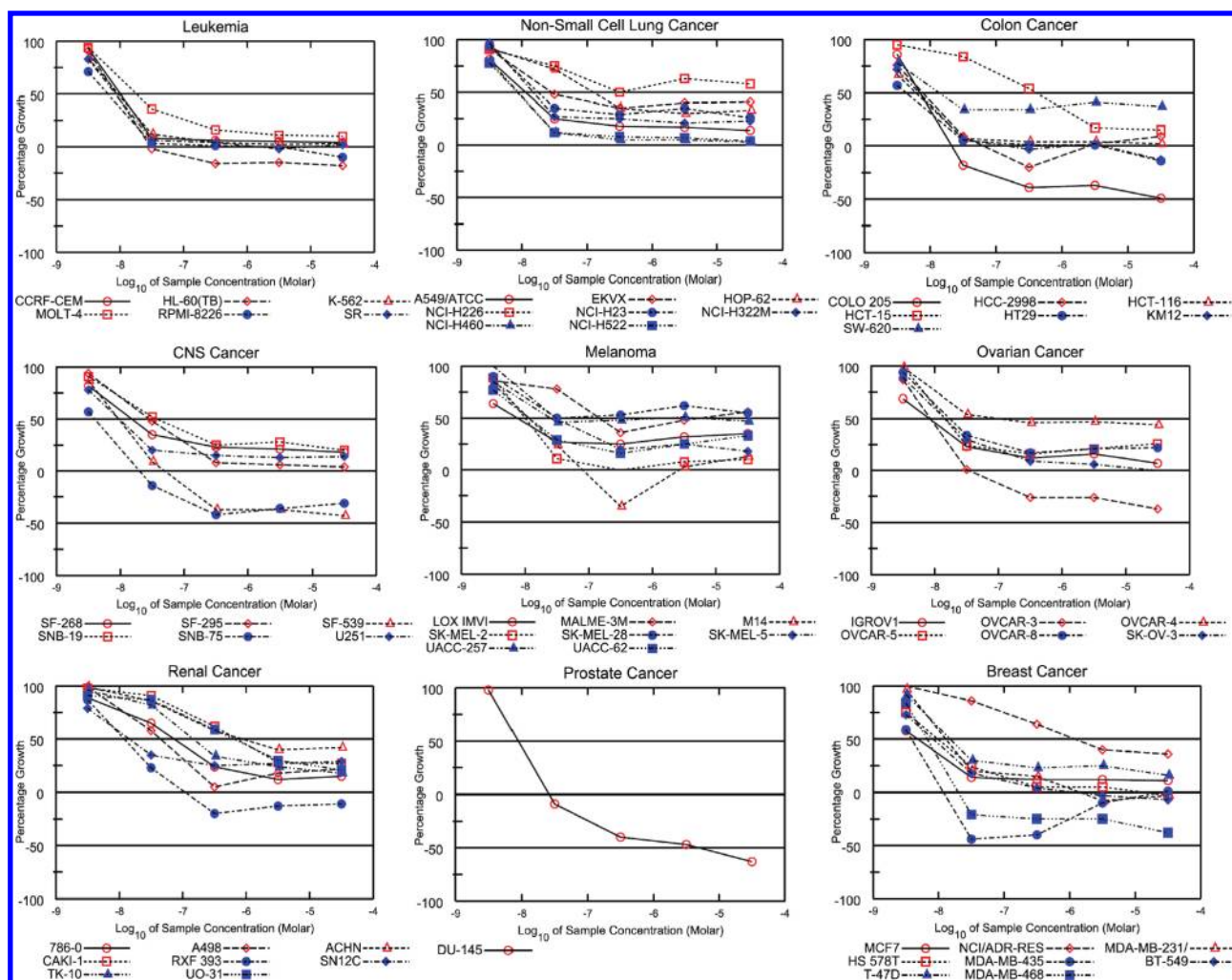
Figure 2. Effects of **1** on the growth of cultured cancer cells performed by NCI. Cells were treated in 96-well plates with five different concentrations of **1** or vehicle. The values for percentage growth of **1**-treated cells compared with those vehicle-treated cells were determined by sulforhodamine-B assay as described in the Experimental Section.

Table 1. Effects of 1 in Female Crl:Nu/Nu Mouse Xenograft Models

xenograft model	dose of **1** (mg/kg)	dosing regimen[a]	% tumor growth inhibition[b]	P
MDA-MB-231	10	q.d. × 24	37.3 (d 25)	<0.05
	15	q.d. × 24	57.4 (d 25)	<0.05
	20	q.d. × 24	72.2 (d 25)	<0.01
	30	q.d. × 12	87.0 (d 25)	<0.001
MCF-7	30	q.d. × 12	100 (d 36)	<0.001
A2780	30	q.d. × 12	45.2 (d 25)	<0.05
ES-2	30	q.d. × 12	36.4 (d 21)	<0.05
H460	5	q.d. × 24	2.15 (d 25)	>0.05
	10	q.d. × 24	17.3 (d 25)	>0.05
	20	q.d. × 24	52.9 (d 25)	<0.01
A549	30	q.d. × 12	79.9 (d 25)	<0.01
H1975	30	q.d. × 12	93.1 (d 25)	<0.001

[a] q.d. means once a day. [b] Tumor growth inhibition was calculated with the following formula: $GI = [(C - T)/C] \times 100$ (C, tumor weight of control group; T, tumor weight of treated group).

and 45.9% (10 mg/kg), respectively. Paclitaxel (3 mg/kg) comparally exhibited 30.5% inhibiton as positive control (Figure 5B). **1** at all doses given, but not paclitaxel, significantly

decreased metastasis nodule counts in lungs of mice, compared to the vehicle control group ($p < 0.01$) (Figure 5C and Figure 5D). Most interestingly, **1** was also significantly superior
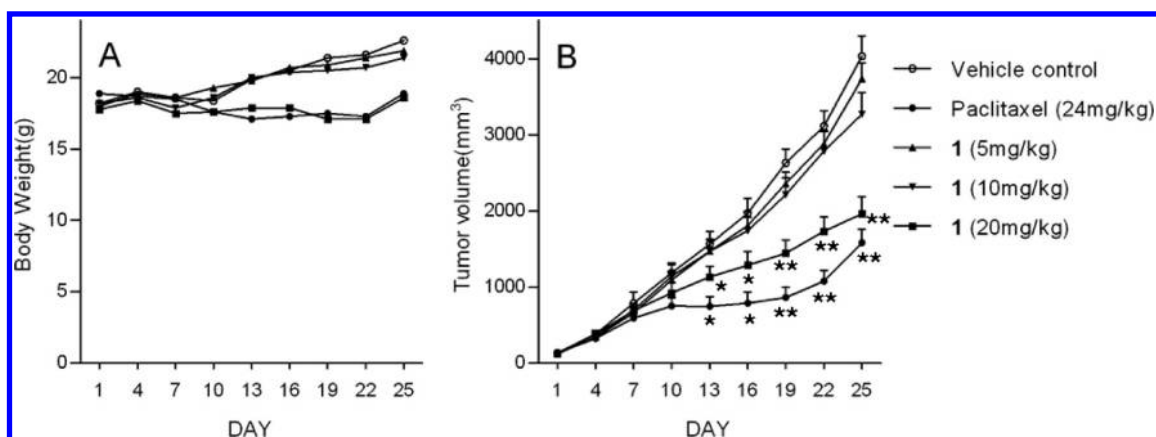
Figure 3. Effects of **1** on body weight (A) and tumor volume (B) of Crl:Nu/Nu mice bearing H460 xenografts. H460 tumors were established in nude mice. When the average tumor volume reached 100 mm^3, intraperitoneal (ip) doses of **1** were delivered at 5, 10, or 20 mg/kg daily for 24 days. The ip injection of paclitaxel (24 mg/kg) was given on days 1, 4, 7, and 10 as a positive control. Data are the mean from one experiment carried out on 10 mice. Error bars represent SEM: (∗) $p < 0.05$ vs vehicle group.
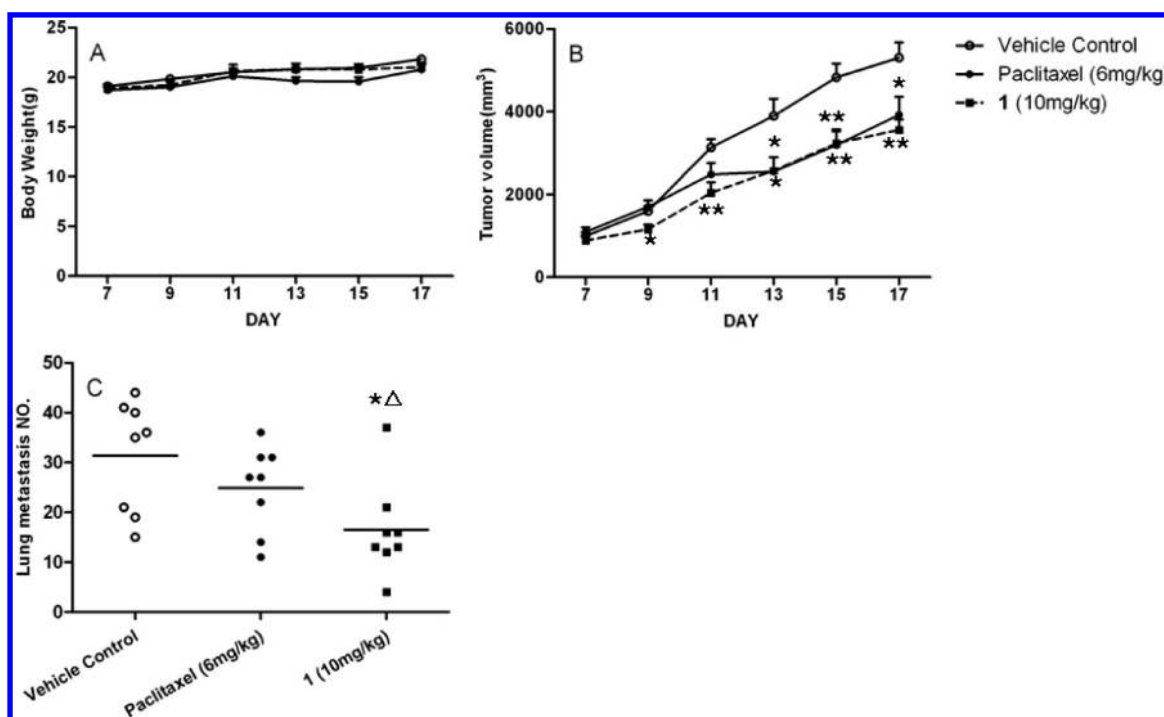

Figure 4. Antitumor and antimetastatic effects of **1** in the LLC model. LLC cells were subcutaneously implanted into the right flank region of C57BL/6 mice (8 mice in each group). **1** or paclitaxel was administered ip at a dose of 10 or 6 mg/kg everyday from day 3 (3 days after cancer cell transplantation) to day 17. The mice were analyzed for body weight (A) and tumor growth (B). At the end of the experiment, lungs were isolated, fixed, and analyzed for the number of lung metastases (C). Error bars represent SEM: (∗) $p < 0.05$, (∗∗) $p < 0.01$ vs vehicle group; (△) $p < 0.05$ vs paclitaxel group.

to paclitaxel treatment in preventing metastasis ($p < 0.01$) (Figure 5C and Figure 5D).

1 Suppresses Myeloid Derived Suppressor Cells (MDSCs) Accumulation in the Spleen and Bone Marrow of 4T1-Tumor-Bearing Mice. To further characterize the effects of **1** in a metastatic tumor model, BALB/c mice were injected in the mammary fat pads with 4T1 cells and were randomly assigned to one of three treatment groups (five mice in each group): vehicle control, paclitaxel (3 mg/kg), or **1** (5 mg/kg). Treatments were given daily starting on day 5 and lasting for 23 days.

After 28 days of tumor growth, accumulation of MDSCs and tumor burden and metastasis were observed in mice of the control group. Representative dot plots are shown above (Figure 6, left). MDSCs made up 52.0% of the spleen cells in untreated controls (Figure 6, right), but a significant drop to 22.0% was observed in the **1**-treated group in comparison to paclitaxel (46.7%). We further examined the bone marrow to determine whether the influence of **1** on MDSCs is widespread. MDSCs normally make up 44.3% of cells in the bone marrow (Figure 6, right), compared with 71.9% in tumor-bearing mice, an increase of approximately 1.6-fold. Again, **1** (45.3%), but not
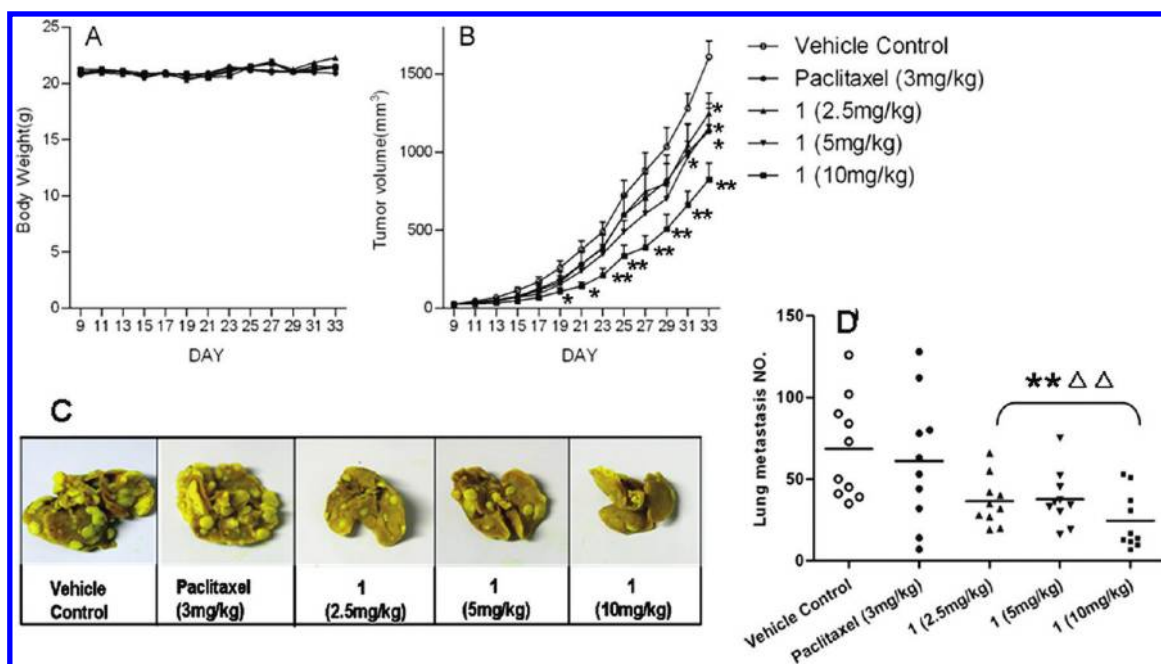
Figure 5. In vivo antitumor and antimetastatic effects of **1** in the 4T1 model. 4T1 cells were transplanted orthotopically to the mammary fat pads of female BALB/c mice (10 mice in each group). Five days after transplantation, mice received ip treatment with **1** (2.5, 5, or 10 mg/kg), paclitaxel (3 mg/kg), or vehicle every day for 28 days and were then analyzed for body weight (A) and tumor growth (B). At the end of the treatment, lungs were isolated, fixed (C), and analyzed for the number of lung metastases (D). The bars represent SEM (A, B): (∗) $p < 0.05$, (∗∗) $p < 0.01$ vs vehicle group; (△) $p < 0.05$, (△△) $p < 0.01$ vs paclitaxel group.
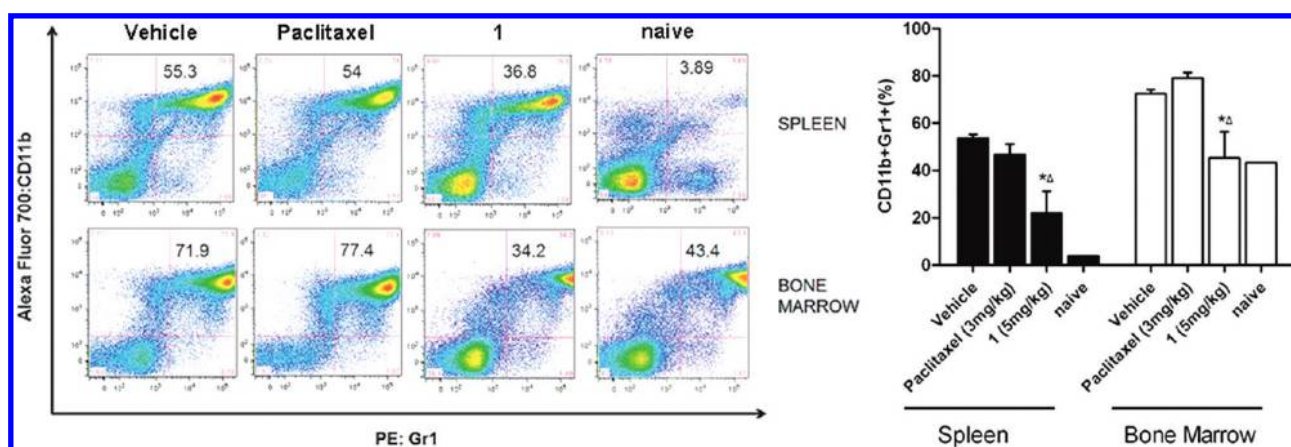

Figure 6. Cells from naive or tumor-bearing mice with different treatments were tested for the expression of CD11b and Gr-1 (to identify the MDSC population). Representative dot plots are shown above (left). Numbers in dot plots indicate the percentage of Gr-1+CD11b+ cells. Bar graphs represent the average of five mice per treatment group or three mice in the naive group (right). Data are expressed as the mean ± SEM: (∗) $p < 0.05$ vs vehicle group; (△) $p < 0.05$ vs paclitaxel group.

paclitaxel (79.1%), significantly prevented MDSC's accumulation in bone marrow. In conclusion, **1** significantly decreased MDSC development in the bone marrow and in the spleen of tumor-bearing mice.

1 Suppresses Inflammatory Cytokines in Tumor Tissue of 4T1-Tumor-Bearded Mice. Because it has been increasingly recognized that the tumor microenvironment plays an important role in tumor metastasis,[24] we meseared the mRNA level for several important metastasis-promoting factors in tumor tissue of 4T1 tumor-bearing mice. As indicated in Figure 7, the expressions of TNF-α, chemokine ligand 2 (CCL2), transforming

growth factor (TGF)-β, and matrix metalloproteinase 9 (MMP9) in tumor tissue were all reduced after **1** treatment.

■ DISCUSSIONS

Over the past decade, paclitaxel has emerged as an effective antitumor agent in a variety of malignancies, including lung, ovarian, and breast cancer.[25] Currently, paclitaxel is semisynthetic but was originally derived from extracts of the Pacific yew tree *Taxus brevifolia*.[4] It binds to microtubules and enhances tubulin polymerization, leading to microtubule stabilization and thereby resulting in the inhibition of cell division.[26] This agent
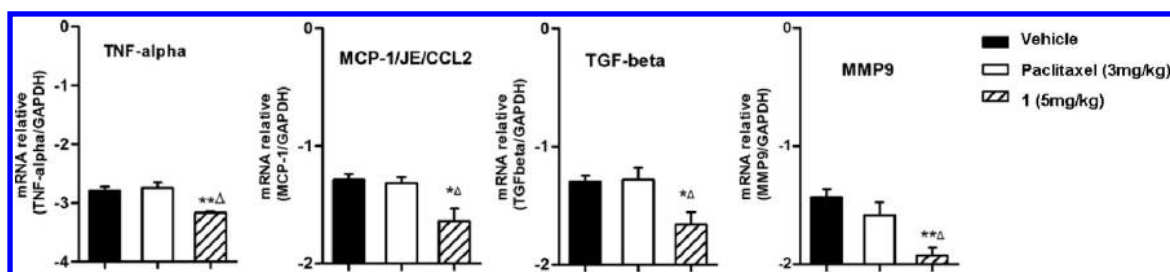
Figure 7. Effects of **1** on the expression of TNF-α or other factors in the tumor tissue of mice. The mRNA level of TGF-β or other inflammatory factors was determined by real-time polymerase chain reaction (PCR). Each value represents the mean ± SEM for five samples: (∗) $p < 0.05$, (∗∗) $p < 0.01$ vs vehicle group; (△) $p < 0.05$, (△△) $p < 0.01$ vs paclitaxel group.

also induces apoptosis by binding to and blocking the function of the apoptosis inhibitor protein Bcl-2 (B-cell leukemia 2).[27]

In parallel, paclitaxel has been reported to activate murine macrophages as a lipopolysaccharide (LPS) mimic, resulting in the secretion of inflammatory mediators including TNF-α, IL-6, and IL-8 in a TLR4-dependent manner.[6,7] Byrd-Leifer[28] and his colleagues reported that paclitaxel and LPS not only share a TLR4/myeloid differentiation primary response gene 88 (MyD88) dependent pathway but also share a TLR4-dependent/MyD88-independent pathway that leads to the activation of mitogen-activated protein kinases (MAPK) and nuclear factor (NF) κB. The interaction of CD14,CD11b/CD18 and heat shock protein 90 is also involved in paclitaxel-induced signaling.[29]

Some investigators have argued that the immunomodulatory effect of paclitaxel only occurs with murine macrophages.[30] However, the demonstration that paclitaxel induces TNF-α, IL-1, and COX-2 in human monocytes;[11,31,32] IL-8 in human tumors;[33] and IL-8, IP-10, or COX-2 in human tumor cell lines[34,35] dispelled this criticism. Moreover, a large amount of evidence suggests that the proinflammatory cytokines produced by paclitaxel may facilitate cancer cells to progress, metastasize, and acquire resistance to chemotherapy.[13−15] These findings have indicated the urgent need for the development of novel strategies for paclitaxel-based therapy of drug-resistant and metastatic cancer.

Using our novel synthetic method on a solid support[22] and the previously described combinatorial technology,[36] we are able to efficiently synthesize large numbers of MTCs in a short period. **1** is identified as a novel antitumor growth and metastasis agent. In vitro and in vivo tests demonstrated that **1** retains its ability to inhibit tumor growth and is superior to paclitaxel because it can also prevent tumor metastasis in LLC and 4T1-tumor-bearing mice.

As mentioned previously, metastasis is the final stage in tumor progression and is thought to be responsible for up to 90% of deaths associated with solid tumors.[1] Metastasis is a complex and multistage process that requires cancer cells to escape from the primary tumor, survive in the circulation, seed at distant sites and grow.[37] A number of studies have indicated that metastasis depends not only on the intrinsic properties of tumor cells but also on the microenvironment from which they derive.[38] Inflammatory components are present in this microenvironment and make a major contribution to tumor metastasis. Key features of cancer-related inflammation include leukocyte infiltration, prominent tumor- associated macrophages and MDSCs, the presence of cytokines such as TNF-α, growth factors such as TGF-β, chemokines such as CCL2, and the occurrence of angiogenesis and tissue remodeling.[39]

In the present study, we found that **1** could significantly suppress MDSC accumulation in tumor-bearing mice. MDSCs are commonly found in many patients and experimental animals with cancer.[40,41] They can accumulate to very high levels in the spleen and bone marrow of a tumor-bearing individual. Recent studies have demonstrated a close correlation between the level of MDSCs and cancer stage, metastatic tumor burden, and responsiveness to chemotherapy.[42] MDSC, characterized as CD11b+Gr-1+ in mice, can be induced by tumor-derived cytokines and growth factors. In particular, the CCL2/CCR2 pathway has been demonstrated to play a critical role in the migration of MDSCs to tumors.[43] Accumulation of MDSCs suppresses both adaptive immune responses and innate immune responses by modulating proinflammatory cytokines and thus directly facilitates metastasis.[44] Evidence has shown that MDSCs can increase production of MMP9,[45] which promotes tumor angiogenesis. They also contribute to TGF β-mediated metastasis through enhancement of tumor cell invasion and migration.[46] TNF-α, another key cytokine linking inflammation and cancer, contributes to the development of the tissue architecture necessary for tumor growth and metastasis. It also induces other cytokines, angiogenic factors, and MMPs and thus leads to the increased growth and survival of tumor cells.[47]

Since **1** sufficiently suppresses MDSCs accumulation in the spleen and bone marrow of a tumor-bearing host and decreases the mRNA levels for TNF-α, TGF-β, CCL2, and MMP9 in the tumor tissue, it is reasonable to conclude that the possible mechanism of the antimetastatic activity of **1** is closely associated with reversal of the inflammatory tumor microenvironment. However, how **1** treatment leads to the adjustment of the tumor microenvironment and the pathway involved remains unclear. One plausible explanation is that **1** may block the TLR4 signaling pathway in cancer cells because **1** is still bearing the paclitaxel motif. Further studies on the inflammatory pathway would be of great interest. As evidenced from the above results, **1** may be a powerful candidate for development of therapeutic and preventive agents for cancer growth and metastasis.

■ EXPERIMENTAL SECTION

Chemistry. All chemical reagents and solvents used were of commercial grade unless otherwise specified. Rink amide-AM resin (cross-linking, 1% DVB; particle size, 100−200 mesh; substitution, 0.88 mmol/g) was purchased from Tianjin Nankai Hecheng Science and Technology Co. Ltd. (China). HPLC analysis was performed on an analytical HPLC system of Agilent Techonologies 1200 series. The employed column was a Kromasil C_{18}, 5 μm, 250 mm × 4.6 mm column from DIKMA (China). The eluent was a mixture of ACN (B) and H_2O

(A) containing 0.05% HCOOH, with a linear gradient elution program from 5% to 95% eluent B within 25 min at a 1.0 mL/min flow rate. The detection was carried out at UV wavelengths of 254 nm. HPLC purification was performed on a Gilson preparative HPLC. Melting points were uncorrected and measured using a Yanaco MP-J3 micromelting point apparatus (Japan). Optical rotation was measured using a model 341LC polarimeter (Perkin-Elmer). All NMR experiments were carried out on a Varian Mercury 300, 500, or 600 MHz NMR spectrometer (Palo Alto, CA). Chemical shifts were reported in ppm (δ) relative to the solvent signal, and coupling constants (J) were reported in Hz. IR spectra were recorded on a Nicolet Impact 400 (San Jose, CA). High resolution LC−MS was performed by Agilent Technologies LC/MSD TOF using a column of Agilent ZORBAX SB-C$_{18}$ (rapid resolution, 3.5 μm, 30 mm × 2.1 mm) at a flow of 0.4 mL/min. The solvent was MeOH/H$_2$O = 75:25 (v:v) containing 0.1% HCOOH. The ion source is electrospray ionization (ESI). All the synthetic compounds reported in this article possess a purity of at least 95%, which are all identified through HPLC analysis (Supporting Information).

Preparation of Fmoc-isoGln-OH (5). To a vigorously stirred solution of D-glutamic acid (2) (29.4 g, 1.0 equiv) in a mixture of acetone and H$_2$O with an equal volume ratio in a water−ice bath, NaHCO$_3$ (18.5 g, 1.1 equiv) and Fmoc-OSu (67.4 g, 1.0 equiv) were added slowly and reacted for an additional 3 days at rt. The mixture was then cooled in a water−ice bath again, and 2.0 N HCl was carefully added until pH 2−3 was attained. After removal of acetone under reduced pressure, the remaining solution was successfully extracted with EtOAc (400 mL, 3 times). The organic layer was separated and combined, dried with MgSO$_4$ overnight, and concentrated to a small volume under reduced pressure. Then cyclohexane (600 mL) was added into the remaining solution to suspend the solid. After filtration, 58.9 g of aimed product 3 was obtained as a white solid with a yield of 79%. 3 (58.9 g, 1.0 equiv) was dissolved in anhydrous THF (324 mL). DCC (40.1 g, 1.2 equiv) was then added while stirring in a water−ice bath. The reaction mixture was allowed to warm to rt and stirring was maintained for an additional 10 h to produce 4. The precipitates were filtered off. Dry ammonia gas was then bubbled through the reactants while stirring in a NaCl salt−ice bath. When no more white solid was precipitated after 1.5 h, the reaction was completed. MeOH (300 mL) was added to dissolve the solid. The mixture was cooled in a water−ice bath again. Then 2.0 N HCl was carefully and slowly added until pH 2−3 was attained. The solvent was evaporated to dryness in a vacuum. The resulting solid was dissolved in EtOAc and then washed with diluted HCl, saturated aqueous NaHCO$_3$ solution, and H$_2$O sequentially. The organic layer was separated and combined, dried with MgSO$_4$ overnight, and evaporated in a vacuum. The precipitate was dissolved in DMF (200 mL). DCM (800 mL) was then slowly added, resulting in the anticipated product 5 (37.0 g) as a white solid with a yield of 63%, mp = 204−205 °C, $[\alpha]_{589}^{25}$ −4.2° (c 10.0 mg/mL, DMF). ^{1}H NMR (300 MHz, DMSO-d_6), Fmoc part: δ 7.88 (d, 2H, J = 7.8 Hz, ph-H), 7.72 (m, 2H, ph-H), 7.42 (m, 2H, ph-H), 7.32 (m, 2H, ph-H), 4.27 (m, 2H, CH$_2$), 4.20 (m, 1H, CH). D-Isoglutamine part: δ 7.40 (m, 1H, NH), 7.04 (br s, 1H, CONH$_a$), 7.29 (br s, 1H, CONH$_b$), 3.93 (dd, 1H, J = 13.5 and 8.5 Hz, α-H), 1.73 (m, 1H, β-H$_a$), 1.89 (m, 1H, β-H$_b$), 2.25 (m, 2H, γ-H), 12.08 (br s, 1H, COOH). ^{13}C NMR (125 MHz, DMSO-d_6), Fmoc part: δ 155.9 (OCONH), 143.8 (ph-C), 140.7 (ph-C), 127.6 (ph-CH), 127.0 (ph-CH), 125.3 (ph-CH), 120.0 (ph-CH), 65.6 (CH$_2$), 46.6 (CH). D-Isoglutamine part: δ 173.4 (CONH$_2$), 53.8 (α-C), 27.2 (β-C), 30.4 (γ-C), 173.9 (COOH). HRMS (TOF): observed for 369.1439 $[M + H]^+$, calcd for 369.1445 $[M + H]^+$, C$_{20}$H$_{20}$N$_2$O$_5$.

Synthesis of N^{α}-[4-Chlorocinnamoyl-L-alanyl-D-isoglutaminyl]-L-lysine (MDA, 6). Fmoc protected Rink amide AM resin (100.0 g, 1.0 equiv) was put into a vessel and vacuumed under reduced pressure. After 1 h, dried DCM (500 mL) was added to swell the resin for 45 min. The Fmoc group of resin was next removed with treatment of 20% piperidine/DMF for 1 h at rt, followed by thorough washing with DMF (500 mL) and DCM (500 mL), respectively, three times each. Fmoc-Lys(Boc)-COOH (61.8 g, 1.5 equiv), HOBt (17.8 g, 1.5 equiv), and DIC (20.8 mL, 1.5 equiv) were dissolved in DMF (500 mL), then poured into the vessel, followed by gentle shaking for 8 h at rt. When the Kaiser test was negative, the coupling reaction was completed. After the Fmoc deprotection and washing were repeated, Fmoc-D-isoGln-OH (48.5 g, 1.5 equiv, for 12 h at rt), Fmoc-Ala-OH (41.0 g, 1.5 equiv, for 8 h at rt), and 4-chlorocinnamic acid (24.1 g, 1.5 equiv, for 8 h at rt) were successfully assembled onto the resin, which led to the resin-bound 6. Targeted compound 6 was finally cleaved off the resin by using 90% TFA/H$_2$O for 2 h at rt. The cocktail cleavage solution was concentrated under reduced pressure. Then dried Et$_2$O was added into the residue under cooling conditions by an ice bath, followed by the same procedure repeated three times. Rude product 6 (52.5 g) was obtained after filteration in 96% yield. The aired dried powder was purified and lyophilized to yield final product 6 as a white powder in 98% purity by ODS column chromatography with gradient elution from 5:95 to 50:50 (v:v) MeOH/H$_2$O, mp = 215−217 °C, $[\alpha]_{589}^{25}$ +37.7° (c 11.0 mg/mL, DMF). ^{1}H NMR (600 MHz, DMSO-d_6), lysine part: δ 7.90 (d, 1H, J = 8.4 Hz, NH), 7.10 (s, 1H, CONH$_a$), 7.30 (s, 1H, CONH$_b$), 4.11 (m, 1H, α-H), 1.46 (m, 1H, β-H$_a$), 1.63 (m, 1H, β-H$_b$), 1.27 (m, 2H, γ-H), 1.53 (m, 2H, δ-H), 2.73 (m, 2H, ε-H), 7.75 (br s, 2H, NH$_2$). D-Isoglutamine part: δ 8.21 (d, 1H, J = 8.4 Hz, NH), 6.98 (s, 1H, CONH$_a$), 7.41 (s, 1H, CONH$_b$), 4.14 (m, 1H, α-H), 1.71 (m, 1H, β-H$_a$), 1.97 (m, 1H, β-H$_b$), 2.15 (t, 2H, J = 7.2 Hz, γ-H). Alanine part: δ 8.39 (d, 1H, J = 6.6 Hz, NH), 4.38 (m, 1H, α-H), 1.26 (m, 3H, β-H). 4-Chlorocinnamoyl part: δ 6.75 (d, 1H, J = 15.9 Hz, trans-α-H), 7.39 (d, 1H, J = 15.9 Hz, trans-β-H), 7.57 (d, 2H, J = 8.4 Hz, ph-o-H), 7.47 (d, 2H, J = 8.4 Hz, ph-m-H). ^{13}C NMR (150 MHz, DMSO-d_6), lysine part: δ 173.3 (CONH$_2$), 52.1 (α-C), 31.3 (β-C), 22.4 (γ-C), 26.8 (δ-C), 38.7 (ε-C). D-Isoglutamine part: δ 173.8 (CONH$_2$), 52.2 (α-C), 27.7 (β-C), 31.7 (γ-C), 171.6 (CONH). Alanine part: δ 172.4 (CONH), 48.8 (α-C), 18.1 (β-C). 4-Chlorocinnamoyl part: δ 164.7 (CONH), 122.7 (trans-α-C), 137.6 (trans-β-C), 133.8 (ph-q-C), 129.2 (ph-o-C), 129.0 (ph-m-C), 134.0 (ph-p-C). IR (KBr): 3281.5, 3198.9, 3063.4, 2935.2, 1609.8, 1539.0, 1452.2, 1200.2, 1134.1, 973.6, 821.6, 799.8, 720.2 cm^{-1}. HRMS (TOF): observed for 509.2270 $[M + H]^+$, calcd for 509.2274 $[M + H]^+$, C$_{23}$H$_{33}$ClN$_6$O$_5$.

Conjugation of Building Blocks To Prepare 1. A solution of 2'-succinylpaclitaxel (7) (9.53 g, 1.0 equiv), which was obtained by Deutsch's method,[48] HOSu (1.15 g, 1.0 equiv), and EDC·HCl (1.92 g, 1.0 equiv) in DMSO was stirred at rt for 8 h to produce 8. Then 6 (5.08 g, 1.0 equiv) was added to the solution slowly and the pH value of solution was carefully adjusted to 7−8 by NMM. The reaction was completed after an additional 30 min of stirring at rt. Then water was slowly added to the solution, which precipitated out crude product 1. The filtrate was purified by preparative HPLC with a linear gradient from 50:50 to 95:5 (v:v) ACN/H$_2$O over 15 min at 3 mL/min flow rate at 254 nm UV detected wavelength and lyophilized to give a white product 1 (13.0 g) in 90% yield, mp = 180−181 °C, $[\alpha]_{589}^{25}$ −9.8° (c 10.0 mg/mL, DMF). ^{1}H NMR (600 MHz, DMSO-d_6): paclitaxel part: δ 4.62 (br s, 1H, 1-OH), 5.40 (d, 1H, J = 7.2 Hz, 2-H), 3.56 (d, 1H, J = 7.2 Hz, 3-H), 4.89 (m, 1H, 5-H), 1.62 (m, 1H, 6-H$_a$), 2.30 (m, 1H, 6-H$_b$), 4.10 (m, 1H, 7-H), 4.90 (m, 1H, 7-OH), 6.28 (s, 1H, 10-H), 5.81 (t, 1H, J = 9.0 Hz, 13-H), 1.46 (m, 1H, 14-H$_a$), 1.79 (m, 1H, 14-H$_b$), 0.99 (s, 3H, 16-H), 1.01 (s, 3H, 17-H), 1.75 (s, 3H, 18-H), 1.49 (s, 3H, 19-H), 3.98 (d, 1H, J = 8.4 Hz, 20-H$_a$), 4.01 (d, 1H, J = 8.4 Hz, 20-H$_b$), 2.23 (s, 3H, 4-OCOCH$_3$), 2.09 (s, 3H, 10-OCOCH$_3$), 5.33 (d, 1H, J = 9.0 Hz, 2'-H), 5.52 (t, 1H, J = 8.4 Hz, 3'-H), 9.21 (d, 1H, J = 8.4 Hz, 3'-NH), 7.48 (d, 2H, J = 7.8 Hz, ph-o-H), 7.46 (m, 2H, ph-m-H), 7.54 (m, 1H, ph-p-H), 7.84 (d, 2H, J = 7.2 Hz, NBz-o-H), 7.42 (m, 2H, NBz-m-H), 7.17 (m, 1H, NBz-p-H), 7.97 (d, 2H, J = 7.2 Hz, OBz-o-H), 7.66 (t, 2H, J = 7.2 Hz, OBz-m-H), 7.72 (t, 1H, J = 7.2 Hz, OBz-p-H). Succinic part: δ 2.60 (m, 2H, OCOCH$_2$),

2.35 (m, 2H, CH$_2$CONH). Lysine part: δ 7.81 (m, 1H, NH), 6.95 (s, 1H, CONH$_a$), 7.29 (s, 1H, CONH$_b$), 4.11 (m, 1H, α-H), 1.45 (m, 1H, β-H$_a$), 1.62 (m, 1H, β-H$_b$), 1.32 (m, 2H, γ-H), 1.22 (m, 2H, δ-H), 2.95 (m, 1H, ε-H$_a$), 3.00 (m, 1H, ε-H$_b$), 7.81 (br s, 1H, NH). D-Isoglutamine part: δ8.20 (d, 1H, J = 7.8 Hz, NH), 7.09 (s, 1H, CONH$_a$), 7.29 (s, 1H, CONH$_b$), 4.13 (m, 1H, α-H), 1.68 (m, 1H, β-H$_a$), 1.98 (m, 1H, β-H$_b$), 2.15 (t, 2H, J = 7.8 Hz, γ-H). Alanine part: δ 8.36 (d, 1H, J = 6.6 Hz, NH), 4.39 (m, 1H, α-H), 1.26 (d, 3H, J = 7.2 Hz, β-H). 4-Chlorocinnamoyl part: δ 6.75 (d, 1H, J = 15.6 Hz, trans-α-H), 7.40 (d, 1H, J = 15.6 Hz, trans-β-H), 7.55 (m, 2H, ph-o-H), 7.48 (m, 2H, ph-m-H). ^{13}C NMR (150 MHz, DMSO-d$_6$): paclitaxel part: δ 76.7 (1-C), 74.5 (2-C), 46.1 (3-C), 80.2 (4-C), 83.6 (5-C), 36.5 (6-C), 70.4 (7-C), 57.4 (8-C), 202.3 (9-C), 74.7 (10-C), 133.3 (11-C), 139.4 (12-C), 70.7 (13-C), 34.4 (14-C), 42.9 (15-C), 26.3 (16-C), 21.4 (17-C), 13.9 (18-C), 9.8 (19-C), 75.3 (20-C), 165.2 (2-OCO), 169.6, 22.5 (4-OCOCH$_3$), 168.8, 20.6 (10-OCOCH$_3$), 169.1 (1′-C), 74.4 (2′-C), 54.0 (3′-C), 166.4 (3′-NHCO), 137.3 (ph-q-C), 127.7 (ph-o-C), 128.3 (ph-m-C), 131.5 (ph-p-C), 129.9 (NBz-q-C), 127.4 (NBz-o-C), 129.0 (NBz-m-C), 128.2 (NBz-p-C), 134.3 (OBz-q-C), 129.6 (OBz-o-C), 128.7 (OBz-m-C), 133.5 (OBz-p-C). Succinic part: δ 172.0 (OCO), 28.8 (OCOCH$_2$), 29.5 (CH$_2$CONH), 170.0 (CONH). Lysine part: δ 173.9 (CONH$_2$), 52.3 (α-C), 31.6 (β-C), 22.9 (γ-C), 28.7 (δ-C), 38.5 (ε-C). D-Isoglutamine part: δ 173.3 (CONH$_2$), 52.1 (α-C), 27.7 (β-C), 31.7 (γ-C), 171.5 (CONH). Alanine part: δ 172.3 (CONH), 48.8 (α-C), 18.1 (β-C). 4-Chlorocinnamoyl part: δ 164.7 (CONH), 122.7 (trans-α-C), 137.6 (trans-β-C), 133.8 (ph-q-C), 129.2 (ph-o-C), 129.0 (ph-m-C), 133.9 (ph-p-C). IR (KBr): 3316.9, 3066.0, 2935.0, 2873.1, 1736.0, 1655.0, 1537.3, 1492.9, 1451.7, 1371.8, 1241.5, 980.2, 906.6, 822.6, 776.2, 708.9 cm^{-1}. HRMS (TOF): observed for 1444.5590 [M + H]$^+$, calcd for 1444.5638 [M + H]$^+$, C$_{74}$H$_{86}$ClN$_7$O$_{21}$.

Biology. Animals. Female C57BL-6J mice (6−7 weeks old), BALB/c mice (6−7 weeks old), ICR mice (6−7 weeks old), and BALB/c nu/nu mice (4−5 weeks old) were obtained from the Experimental Animal Center, Chinese Academy of Medical Sciences and Peking Union Medical College (SPF, Certificate No. SCXK 2005-0013). All animals were housed in groups under a 12:12 h regime (lights on from 7:00 to 19:00) at 23 ± 2 °C prior to the experiments and were given standard laboratory chow and tap water ad libitum.

NCI 60 Cancer Cell Line Screen. 1 was screened through the National Cancer Institute (NCI) Developmental Therapeutics Program (DTP) 60 human cancer cell line panel under the In Vitro Cell Line Screening Project (IVCLSP).[49] Briefly, cells (5000 to 40 000 cells/well depending on the cell line studied) were inoculated into 96-well microtiter plates in 100 μL of complete RPMI1640 medium (5% FBS and 2 mM L-glutamine) and incubated 24 h prior to addition of 1. 1 was added, and the plates were incubated at 37 °C, 5% CO$_2$, 95% air, and 100% relative humidity for an additional 48 h. Upon the addition of 50 μL of cold TCA (10% TCA) the assay was terminated and incubated for 60 min at 4 °C to fix the cells. The supernatant was discarded, and the plates were washed five times with water and air-dried. Sulforhodamine B solution (100 μL) at 0.4% (v/v) in 1% acetic acid was added to each well, and plates were incubated for 10 min at room temperature. After staining, unbound dye was removed by washing five times with 1% acetic acid and the plates were air-dried. Bound stain was subsequently solubilized with 10 mM trizma base, and the absorbance was read on an automated plate reader at a wavelength of 515 nm. Using absorbance measurements [time zero (T_z), control growth (C), and test growth in the presence of drug (T_i)], the percentage growth was calculated. Percentage growth inhibition was calculated as $[(T_i − T_z)/(C − T_z)] × 100$ for concentrations for which $T_i ≥ T_z$ and as $[(T_i − T_z)/T_z] × 100$ for concentrations for which $T_i < T_z$.

Mouse Xenograft Studies. Several xenografts models using human breast (MDA-MB-231, MCF-7), ovarian (A2780, ES-2), and lung (H460, A549, H1975) tumor cell lines were established. Generally speaking, tumors were maintained by regular monthly sc transplantations, performed on BALB/c nu/nu mice. At each transfer, tumors were minced into 10 mm^3 pieces and sc inoculated on the right flank by means of a trocar. Tumor fragments (diameter for about 3 mm) from in vivo passage were implanted into the axillary region of the mice. Tumors were allowed to grow to an average volume of 100 mm^3 before beginning treatment with 1. Tumor growth was measured using vernier calipers to determine two orthogonal axes. Tumor volume is given by the formula $(^1/_2)a^2b$, where a is the shorter axis and b is the longer axis. At the end of the experiment, the primary tumors were removed and weighed. Tumor growth inhibition was calculated by the following formula: $[(C − T)/C] × 100$ (C, tumor weight of control group; T, tumor weight of treated group).

Spontaneous Metastasis Model of LLC. The LLC cell line used was a generous gift from Prof. Nan Wang and was locally maintained in C57Bl/6 mice by serially biweekly passages. The $1 × 10^6$ LLC tumor cells of a single cell suspension, prepared by mincing with scissors the primary tumors from donors implanted 2 weeks previously, were injected subcutaneously into the right hind calf of the mice. Three days after the implantation of LLC tumor cells, the mice were divided randomly into three groups and received intraperitoneal administration of control verhicle, paclitaxel (6 mg/kg), or 1 (10 mg/kg) once daily. Beginning on day 7 after implantation, primary tumor growth was measured using vernier calipers to determine two orthogonal axes. Tumor volume is given by the formula $(^1/_2)a^2b$, where a is the shorter axis and b is the longer axis. Eighteen days after implantation, all mice were sacrificed by cervical dislocation. The primary tumors were removed and weighed. The lungs were removed, weighed, and fixed in Bouin's solution overnight before evaluation of lung metastasis. The number of lung metastases was counted.

4T1 Murine Mammary Carcinoma Model. The mouse mammary gland adenocarcinoma cell line 4T1 was a generous gift from Prof. Wei Liang and was grown in RPMI 1640 medium (Invitrogen Co., Carlsbad, CA) supplemented with 10% fetal bovine serum (FBS) and adjusted to contain 2 mM L-glutamine, 1.5 g/L sodium bicarbonate, 4.5 g/L glucose, 10 mM HEPES, and 1.0 mM sodium pyruvate (Gemini Bio-Products Woodland, CA). 4T1 tumors were induced in female BALB/c mice by injecting 100 μL of a single-cell suspension ($2 × 10^6$ viable cells/mL) subcutaneously into the fat pad area of the right abdominal mammary gland. Five days after the implantation of 4T1 tumor cells, the mice were divided randomly into five groups and received intraperitoneal administration of control vehicle, paclitaxel (3 mg/kg), or 1 (2.5, 5, or 10 mg/kg) once daily. Beginning on day 7 after implantation, primary tumor growth was measured every 2 days using vernier calipers to determine the two orthogonal axes. Tumor volume is given by the formula $(^1/_2)a^2b$, where a is the shorter axis and b is the longer axis. Twenty-eight days after implantation, all mice were then sacrificed by cervical dislocation. The primary tumors were removed and weighed. The lungs were removed, weighed, and fixed. The number of lung metastases was counted.

Flow Cytometry Analysis. Spleens are harvested and crushed through a cell strainer. Femurs from mice are collected and flushed with complete RPMI to collect bone marrow. After lysis of erythrocytes, the remaining cells are washed twice with 1× PBS, brought to $1 × 10^6$/100 mL, and stained for 30 min with anti-mouse CD11b (AF700-conjugated) and anti-mouse Ly-6G/Ly-6C (Gr-1) (PE-conjugated) (Biolegend, San Diego, CA). Unstained cells were used as a negative control, and rat IgG2bκ was used as the isotype control. Staining with CD11b alone or Gr-1 alone was used as single color positive controls. Stained cells were fixed with 2% paraformaldehyde and analyzed (30 000 cells per sample) within 7 days of staining. For flow cytometry analysis, a large forward scatter/side scatter gate was drawn to include lymphocyte/monocyte population. Then samples were analyzed with flow cytometer (LSR, BD).

Quantitative Real Time RT-PCR. Tumor tissue was lysed in TRIzol, and total RNA was extracted with an RNeasy minikit (Qiagen). An amount of 100 ng of RNA was transcribed into cDNA with random hexamer. Real time RT-PCR was carried out on the ABI PRISM 7900HT sequence detection system (PerkinElmer). The primer sequences for cytokine in real time RT-PCR are as follows: TNF-α, forward primer TGC TTG TTG ACA GCG GTC C, reverse primer ACT GGC CAT CGT GGA GGT AC, and probe AGG GCA GTG TGT TAC GTG CAG TGA CAA; CCL-2, forward primer GAG CAT CCA CGT GTT GGC T, reverse primer TGG TGA ATG AGT AGC AGC AGG T, and probe AGC CAG ATG CAG TTA ACG CCC CAC T; TGF-β, forward primer GCC ACT GCC CAT CGT CTA, reverse primer GAG CGC ACA ATC ATG TTG GA, and probe CTA CGT GGG TCG CAA GCC CAA G; MMP9, forward primer CGC GTG GAT AAG GAG TTC TC, reverse primer CCA TGG CAG AAA TAG GCT TTG TC, and probe TGG TGT GCC CTG GAA CTC ACA. The amount of mRNA was expressed as copies of mRNA per copy of GAPDH mRNA.

Statistical Analyses. Statistical analyses were done using the two-tailed Student's *t* test for independent samples. *P* < 0.05 was considered statistically significant. All the data are presented as the mean ± SEM.

■ ASSOCIATED CONTENT

ⓢ Supporting Information. NMR spectra; HR-MS and IR results of Fmoc-iso-Gln-OH, MDA, and **1**; HPLC analysis profiles of Fmoc-iso-Gln-OH and MDA at the UV wavelengths of 254 and 214 nm; HPLC analysis profiles of **1** at 214 nm UV wavelength; and table of IC$_{50}$ values of **1** on tumor cells. This material is available free of charge via the Internet at http://pubs.acs.org.

■ AUTHOR INFORMATION

Corresponding Author
*Phone: 86-10-63167165. Fax: 86-10-63165246. E-mail: gliu@imm.ac.cn.

Author Contributions
[†]These authors contributed equally to this work.

■ ACKNOWLEDGMENT

■ ABBREVIATIONS USED

ACN, acetonitrile; Bcl-2, B-cell leukemia 2; CCL, chemokine ligand; COX-2, cyclooxygenase-2; DCC, dicyclohexylcarbodiimide; DCM, dichlormethane; DIC, *N,N'*-diisopropylcarbodiimide; DMF, *N,N'*-dimethylformamide; DMSO, dimethylsulfoxide; EDC·HCl, 1-(3-dimethylaminopropyl)-3-ethylcarbodiimide hydrochloride; Et$_2$O, ethyl ether; EtOAc, ethyl acetate; EFS, even-free survival; Fmoc, 9-fluorenylmethoxycarbonyl; HOBt, 1-hydroxybenzotriazole; HOSu, *N*-hydroxysuccinimide; HPLC, high performance liquid chromatography; HR-MS, high resolution mass spectra; IR, infrared (spectra); LC/TOF-MS, liquid chromatography/time-of-flight mass spectra; LLC, Lewis lung carcinoma; LPS, lipopolysaccharide; MAPK, mitogen-activated protein kinases; MDA, muramyl dipeptide analogue; MDP, muramyl dipeptide; MDSC, myeloid derived suppressor cell; MMP9, matrix metalloproteinase 9; NF, nuclear factor; MeOH, methanol; mp, melting point; NMM, *N*-methylmorpholine; NMR, nuclear magnetic resonance; ODS, octadecylsilane; PCR, polymerase chain reaction; rt, room temperature; TFA, trifluoroacetic acid; TGF, transforming growth factor; THF, tetrahydrofuran; TLR, Toll-like receptor; TNF, tumor necrosis factor

■ REFERENCES

(1) Gupta, G. P.; Massagué, J. Cancer metastasis: building a framework. *Cell* **2006**, *127*, 679–695.

(2) Steeg, P. S. Tumor metastasis: mechanistic insights and clinical challenges. *Nat. Med.* **2006**, *12*, 895–904.

(3) Meyers, P. A. Muramyl tripeptide (mifamurtide) for the treatment of osteosarcoma. *Expert Rev Anticancer Ther.* **2009**, *9*, 1035–1049.

(4) Meyers, P. A.; Schwartz, C. L.; Krailo, M.; Kleinerman, E. S.; Betcher, D.; Bernstein, M. L.; Conrad, E.; Ferguson, W.; Gebhardt, M.; Goorin, A. M.; Harris, M. B.; Healey, J.; Huvos, A.; Link, M.; Montebello, J.; Nadel, H.; Nieder, M.; Sato, J.; Siegal, G.; Weiner, M.; Wells, R.; Wold, L.; Womer, R.; Grier, H. Osteosarcoma: a randomized, prospective trial of the addition of ifosfamide and/or muramyl tripeptide to cisplatin, doxorubicin, and high-dose methotrexate. *J. Clin. Oncol.* **2005**, *23*, 2004–2011.

(5) Wani, M. C.; Taylor, H. L.; Wall, M. E.; Coggon, P.; McPhail, A. T. Plant antitumor agents. VI. Isolation and structure of Taxol, a novel antileukemic and antitumor agent from *Taxus brevifolia*. *J. Am. Chem. Soc.* **1971**, *93*, 2325–2327.

(6) Schiff, P. B.; Horwitz, S. B. Taxol stabilizes microtubules in mouse fibroblast cells. *Proc. Natl. Acad. Sci. U.S.A.* **1980**, *77*, 1561–1565.

(7) Kawasaki, K.; Akashi, S.; Shimazu, R.; Yoshida, T.; Miyake, K.; Nishijima, M. Mouse Toll-like receptor 4. MD-2 complex mediates lipopolysaccharide-mimetic signal transduction by Taxol. *J. Biol. Chem.* **2000**, *275*, 2251–2254.

(8) Ding, A. H.; Porteu, F.; Sanchez, E.; Nathan, C. F. Shared actions of endotoxin and Taxol on TNF receptors and TNF release. *Science* **1990**, *248*, 370–372.

(9) Kim, S.; Takahashi, H; Lin, W. W.; Descargues, P.; Grivennikov, S.; Kim, Y.; Luo, J. L.; Karin, M. Carcinoma-produced factors activate myeloid cells through TLR2 to stimulate metastasis. *Nature* **2009**, *457*, 102–106.

(10) Balkwill, F. TNF-α in promotion and progression of cancer. *Cancer Metastasis Rev.* **2006**, *25*, 409–416.

(11) Allen, J. N.; Moore, S. A.; Wewers, M. D. Taxol enhances but does not induce interleukin 1 beta and tumor necrosis factor alpha production. *J. Lab. Clin. Med.* **1993**, *122*, 374–381.

(12) Wang, J.; Kobayashi, M.; Han, M.; Choi, S.; Takano, M.; Hashino, S.; Tanaka, J.; Kondoh, T.; Kawamura, K.; Hosokawa, M. MyD88 is involved in the signalling pathway for Taxol induced apoptosis and TNF-α expression in human myelomonocytic cells. *Br. J. Haematol.* **2002**, *118*, 638–645.

(13) Lee, L. F.; Schuerer-Maly, C. C.; Lofquist, A. K.; van Haaften-Day, C.; Ting, J. P.; White, C. M.; Martin, B. K.; Haskill, J. S. Taxol dependent transcriptional activation of IL-8 expression in a subset of human ovarian cancer. *Cancer Res.* **1996**, *56*, 1303–1308.

(14) Wang, A. C.; Su, Q. B.; Wu, F. X.; Zhang, X. L.; Liu, P. S. Role of TLR4 for paclitaxel chemotherapy in human epithelial ovarian cancer cells. *Eur. J. Clin. Invest.* **2009**, *39*, 157–164.

(15) Szajnik, M.; Szczepanski, M. J.; Czystowska1, M.; Elishaev, E.; Mandapathil, M.; Nowak-Markwitz, E.; Spaczynski, M.; Whiteside1,

T. L. TLR4 signaling induced by lipopolysaccharide or paclitaxel regulates tumor survival and chemoresistance in ovarian cancer. *Oncogene* **2009**, *28*, 4353–4363.

(16) He, W.; Liu, Q.; Wang, L.; Chen, W.; Li, N.; Cao, X. TLR4 signaling promotes immune escape of human lung cancer cells by inducing immunosuppressive cytokines and apoptosis resistance. *Mol. Immunol.* **2007**, *44*, 2850–2859.

(17) Tsavaris, N.; Kosmas, C.; Vadiaka, M.; Kanelopoulos, P.; Boulamatsis, D. Immune changes in patients with advanced breast cancer undergoing chemotherapy with taxanes. *Br. J. Cancer* **2002**, *87*, 21–27.

(18) Ellouz, F.; Adam, A.; Ciorbaru, R.; Lederer, E. Minimal structural requirements for adjuvant activity of bacterial peptidoglycan derivatives. *Biochem. Biophys. Res. Commun.* **1974**, *59*, 1317–1325.

(19) Adam, A.; Ciorbaru, R.; Ellouz, F.; Petit, J. F.; Lederer, E. Adjuvant activity of monomeric bacterial cell wall peptidoglycans. *Biochem. Biophys. Res. Commun.* **1974**, *56*, 561–567.

(20) Parant, M. A.; Audibert, F. M.; Chedid, L. A.; Level, M. R.; Lefrancier, P. L.; Choay, J. P.; Lederer, E. Immunostimulant activities of a lipophilic muramyl dipeptide derivative and of desmuramyl peptido-lipid analogs. *Infect. Immun.* **1980**, *27*, 826–831.

(21) Riveau, G. J.; Brunel-Riveau, B. G.; Audibert, F. M.; Chedid, L. A. Influence of a muramyl dipeptide on human blood leukocyte functions and their membrane antigens. *Cell. Immunol.* **1991**, *134*, 147–156.

(22) Li, X.; Yu, J.; Xu, S; Wang, N.; Yang, H.; Yan, Z.; Cheng, G.; Liu, G. Chemical conjugation of muramyl dipeptide and paclitaxel to explore the combination of immunotherapy and chemotherapy for cancer. *Glycoconjugate J.* **2008**, *25*, 415–425.

(23) Liu, G; Cheng, G; Wang, N; Li, X; Yu, J; Xu, S; Fang, Q. Conjugation of Muramyl Dipeptide and Paclitaxel. P. R. China Patent ZL200510081265.X, 2005.

(24) Joyce, J. A.; Pollard, J. W. Microenvironmental regulation of metastasis. *Nat. Rev. Cancer* **2009**, *9*, 239–252.

(25) Grown, J.; O' Leary, M. The taxanes: an update. *Lancet* **2000**, *355*, 1176–1178.

(26) Horwitz, S. B.; Lothstein, L.; Manfredi, J. J.; Mellado, W.; Parness, J.; Roy, S. N.; Schiff, P. B.; Sorbara, L.; Zeheb, R. Taxol: mechanisms of action and resistance. *Ann. N.Y. Acad. Sci.* **1986**, *466*, 733–744.

(27) Bhalla, K.; Ibrado, A. M.; Tourkina, E.; Tang, C.; Mahoney, M. E.; Huang, Y. Taxol induces internucleosomal DNA fragmentation associated with programmed cell. *Leukemia* **1993**, *7*, 563–568.

(28) Byrd-Leifer, C. A.; Block, E. F.; Takeda, K.; Akira, S.; Ding, A. The role of MyD88 and TLR4 in the LPS-mimetic activity of Taxol. *Eur. J. Immunol.* **2001**, *31*, 2448–2457.

(29) Fitzpatrick, F. A.; Wheeler, R. The immunopharmacology of paclitaxel (Taxol), docetaxel (Taxotere), and related agents. *Int. Immunopharmacol.* **2003**, *3*, 1699–1714.

(30) Manthey, C. L.; Qureshi, N.; Stutz, P. L.; Vogel, S. N. Lipopolysaccharide antagonists block Taxol-induced signaling in murine macrophages. *J. Exp. Med.* **1993**, *178*, 695–702.

(31) Cassidy, P. B.; Moos, P. J.; Kelly, R. C.; Fitzpatrick, F. A. Cyclooxygenase-2 induction by paclitaxel, docetaxel and taxane analogs in human monocytes and murine macrophages: structure–activity relationships and their implications. *Clin. Cancer Res.* **2002**, *8*, 846–855.

(32) Moos, P. J.; Muskardin, D. T.; Fitzpatrick, F. A. Effect of Taxol and taxotere on gene expression in macrophages: induction of the prostaglandin H synthase-2 isoenzyme. *J. Immunol.* **1999**, *162*, 467–473.

(33) Watson, J. M.; Kingston, D. G.; Chordia, M. D.; Chaudhary, A. G.; Rinehart, C. A.; Haskill, J. S. Identification of the structural region of Taxol that may be responsible for cytokine gene induction and cytotoxicity in human ovarian cancer cells. *Cancer Chemother. Pharmacol.* **1998**, *41*, 391–397.

(34) Subbaramaiah, K.; Hart, J. C.; Norton, L.; Dannenberg, A. J. Microtubule-interfering agents stimulate the transcription of cyclooxygenase-2. Evidence for involvement of ERK1/2 and p38 mitogen-activated protein kinase pathways. *J. Biol. Chem.* **2000**, *275*, 14838–14845.

(35) Zaks-Zilberman, M.; Zaks, T. Z.; Vogel, S. N. Induction of proinflammatory and chemokine genes by lipopolysaccharide and paclitaxel (Taxol) in murine and human breast cancer cell lines. *Cytokine* **2001**, *15*, 156–165.

(36) (a) Liu, G.; Zhang, S. D.; Xia, S. Q.; Ding, Z. K. Solid-phase synthesis of of muramyl dipeptide (MDP) derivatives using a multipin method. *Bioorg. Med. Chem. Lett.* **2000**, *10*, 1361–1363. (b) Yang, H. Z.; Xu, S.; Liao, X. Y.; Zhang, S. D.; Liang, Z. L.; Liu, B. H.; Bai, J. Y.; Jiang, C.; Ding, J.; Cheng, G. F.; Liu, G. A novel immunostimulator, N^2-[α-O-benzyl-N-(acetylmuramyl)-L-alanyl-D-isoglutaminyl]-N^6-*trans*-(*m*-nitrocinnamoyl)-L-lysine (MDP-C), and its adjuvancy on the hepatitis B surface antigen. *J. Med. Chem.* **2005**, *48*, 5112–5122.

(37) Mehlen, P.; Puisieux, A. Metastasis: a question of life or death. *Nat Rev Cancer* **2006**, *6*, 449–458.

(38) Wu, Y.; Zhou, B. P. Inflammation: a driving force speeds cancer metastasis. *Cell Cycle* **2009**, *8*, 3267–3273.

(39) Mantovani, A.; Garlanda, C.; Allavena, P. Molecular pathways and targets in cancer-related inflammation. *Ann. Med.* **2010**, *42*, 161–170.

(40) Almand, B.; Clark, J. I.; Nikitina, E.; van Beynen, J.; English, N. R.; Knight, S. C.; Carbone, D. P.; Gabrilovi, D. I. Increased production of immature myeloid cells in cancer patients: a mechanism of immunosuppression in cancer. *J. Immunol.* **2001**, *166*, 678–689.

(41) Young, M. R.; Lathers, D. M. Myeloid progenitor cells mediate immune suppression in patients with head and neck cancers. *Int. J. Immunopharmacol.* **1999**, *21*, 241–252.

(42) Diaz-Montero, C. M.; Salem, M. L.; Nishimura, M. I.; Garrett-Mayer, E.; Cole, D. J.; Montero, A. J. Increased circulating myeloid-derived suppressor cells correlate with clinical cancer stage, metastatic tumor burden and doxorubicin-cyclophosphamide chemotherapy. *Cancer Immunol. Immunother.* **2009**, *58*, 49–59.

(43) Huang, B.; Lei, Z.; Zhao, J.; Gong, W.; Liu, J.; Chen, Z.; Liu, Y.; Li, D.; Yuan, Y.; Zhang, G. M.; Feng, Z. H. CCL2/CCR2 pathway mediates recruitment of myeloid suppressor cells to cancers. *Cancer Lett.* **2007**, *252*, 86–92.

(44) Sinha, P.; Clements, V. K.; Bunt, S. K.; Albelda, S. M.; Ostrand-Rosenberg, S. Cross-talk between myeloid-derived suppressor cells and macrophages subverts tumor immunity toward a type 2 response. *J. Immunol.* **2007**, *179*, 977–983.

(45) Yang, L.; DeBusk, L. M.; Fukuda, K.; Fingleton, B.; Green-Jarvis, B.; Shyr, Y.; Matrisian, L. M.; Carbone, D. P.; Lin, P. C. Expansion of myeloid immune suppressor Gr+CD11b+ cells in tumor-bearing host directly promotes tumor angiogenesis. *Cancer Cell* **2004**, *6*, 409–421.

(46) Yang, L.; Huang, J.; Ren, X.; Gorska, A. E.; Chytil, A.; Aakre, M.; Carbone, D. P.; Matrisian, L. M.; Richmond, A.; Lin, P. C.; Moses, H. L. Abrogation of TGF-β signaling in mammary carcinomas recruits Gr-1+CD11b+ myeloid cells that promote metastasis. *Cancer Cell* **2008**, *13*, 23–35.

(47) Wu, Y.; Zhou, B. P. TNF-a/NF-kB/Snail pathway in cancer cell migration and invasion. *Br. J. Cancer* **2010**, *102*, 639–644.

(48) Deutsch, H. M.; Glinski, J. A.; Hernandez, M.; Haugwitz, R. D.; Narayanan, V. L.; Suffness, M.; Zalkow, L. H. Synthesis of congeners and prodrugs. 3. Water-soluble prodrugs of Taxol with potent antitumor activity. *J. Med. Chem.* **1989**, *32*, 788–792.

(49) Shoemaker, R. H. The NCI60 human tumour cell line anticancer drug screen. *Nat. Rev. Cancer* **2006**, *6*, 813–823.